

Light propagation in single mode polymer nanotubes integrated on photonic circuits

Nolwenn Huby, Jean Luc Duvail, Daphné Duval, David Pluchon, and Bruno Bêche

Citation: *Appl. Phys. Lett.* **99**, 113302 (2011); doi: 10.1063/1.3637043

View online: <http://dx.doi.org/10.1063/1.3637043>

View Table of Contents: <http://apl.aip.org/resource/1/APPLAB/v99/i11>

Published by the [American Institute of Physics](http://www.aip.org).

Related Articles

Density and birefringence of a highly stable α,α,β -trisnaphthylbenzene glass

J. Chem. Phys. **136**, 204501 (2012)

Molecular orientation and anisotropic carrier mobility in poorly soluble polythiophene thin films

APL: Org. Electron. Photonics **5**, 112 (2012)

Molecular orientation and anisotropic carrier mobility in poorly soluble polythiophene thin films

Appl. Phys. Lett. **100**, 203305 (2012)

Interplay between intrachain and interchain interactions in semiconducting polymer assemblies: The HJ-aggregate model

J. Chem. Phys. **136**, 184901 (2012)

Excitation dynamics of a low bandgap silicon-bridged dithiophene copolymer and its composites with fullerenes

APL: Org. Electron. Photonics **5**, 90 (2012)

Additional information on *Appl. Phys. Lett.*

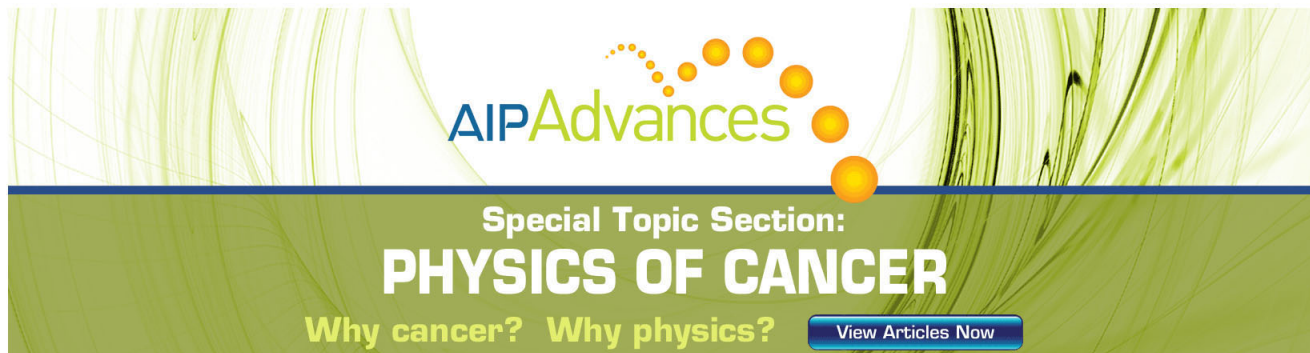
Journal Homepage: <http://apl.aip.org/>

Journal Information: http://apl.aip.org/about/about_the_journal

Top downloads: http://apl.aip.org/features/most_downloaded

Information for Authors: <http://apl.aip.org/authors>

ADVERTISEMENT



AIP Advances

Special Topic Section:
PHYSICS OF CANCER

Why cancer? Why physics? [View Articles Now](#)

Light propagation in single mode polymer nanotubes integrated on photonic circuits

Nolwenn Huby,^{1,a)} Jean Luc Duvail,² Daphné Duval,³ David Pluchon,¹ and Bruno Bêche¹

¹Institut de Physique de Rennes, UMR CNRS 6251, Université de Rennes 1, 263 avenue Général Leclerc, Rennes 35042, France

²Institut des Matériaux, UMR CNRS 6502, Université de Nantes, 2 rue de la Houssinière B.P.32229, 44322 Nantes cedex 3, France

³Nanobiosensors and Bioanalytical Applications Group, CIN2 (CSIC-ICN) and CIBER-BBN, Campus UAB, 08193, Bellaterra, Barcelona, Spain

(Received 15 July 2011; accepted 21 August 2011; published online 13 September 2011)

We report the theoretical and experimental study of photonic propagation in organic dielectric nanotubes elaborated by a wetting template method and showing off an aspect ratio as high as 200. Single mode behaviour is theoretically demonstrated without any cut-off conditions. Efficient evanescent coupling between polymer microstructures and nanotubes dispersed on a photonic chip as well as the high confinement and propagation in a single nanotube have been demonstrated. These results show the potential of well-defined one-dimensional nanostructures as building blocks for integrated organic photonic devices. Applications such as sensing and high speed communication are envisaged. © 2011 American Institute of Physics. [doi:10.1063/1.3637043]

Integrated photonic circuits offer great opportunities for high speed data transport and highly sensitive sensors. Related improvements rely on the comprehension of optical properties at the nanoscale and on the design of densely packed photonic devices. In this context, high aspect ratio nanostructures are mostly interesting. In particular, cylindrical nanostructures (nanowires and nanotubes NTs) always support at least one optical mode whatever their diameter. Moreover, they present a high evanescent field which can be exploited for highly sensitive sensors¹ and for efficient coupling with photonic structures.² Regarding the strategies for integrated photonics found in the literature, the ones based on polymeric materials are of great interest. Indeed, they present a large range of accessible optical properties by modification of their chemical structure. Moreover, liquid-phase processability and flexible support allow a large scale fabrication. Thereby, polymer-based photonic devices have already been reported such as organic light-emitting diodes,³ photodiode,⁴ solar cell,⁵ coupling splitters,⁶ or non-linear waveguides.⁷ Nevertheless, despite the increasing number of reports in nanophotonics involving 1D-nanostructures, dielectric organic nanotubes present a lack of investigations. Only a few in-solution fabrication methods are appropriate for tubular nanostructure elaboration. Among them, the wetting template method⁸ appears quite unique to precisely control the diameters of a large number of nanostructures processed in parallel in a non-consuming time, as evidenced recently for insulating⁹ and semi-conducting polymers.^{10,11}

In this letter, we show photonic waveguiding behaviour in single organic SU8 (epoxy based negative photoresist) nanotube by a theoretical approach supplemented by an experimental investigation. This SU8 material has been already used at a micro-scale as light guiding structures,¹² photonic crystal,¹³ and MEMS¹⁴ thus demonstrating it is an appropri-

ate candidate for integrated optics. Its experimental investigation at the nanoscale is here performed by integrating SU8 nanotubes on a photonic chip also constituted of SU8 waveguiding structures.

The theoretical approach has been performed by applying to dielectric organic nanotubes an original analytical formalism recently developed.¹⁵ The modal cut-off thicknesses of the NTs are obtained by resolving numerically the eigenvalue equations. These cut-off values (outer ϕ_{out} and inner ϕ_{in} diameters) govern the presence or not of a mode in the structure. Figure 1 shows the cut-off values for the transverse electric TE₀₁ and transverse magnetic TM₀₁ modes. The normalized inner diameter ϕ_{in}/λ is plotted as a function of the normalized outer diameter ϕ_{out}/λ resulting in a map of single mode and multimode areas, λ being the wavelength. The geometrical limit depicts the forbidden zone where ϕ_{in} can not exceed ϕ_{out} . The main result is that for ϕ_{out}/λ smaller than 0.64, the structure is single hybrid (HE₁₁) whatever the inner diameter. For larger ϕ_{out}/λ , additional modes are allowed

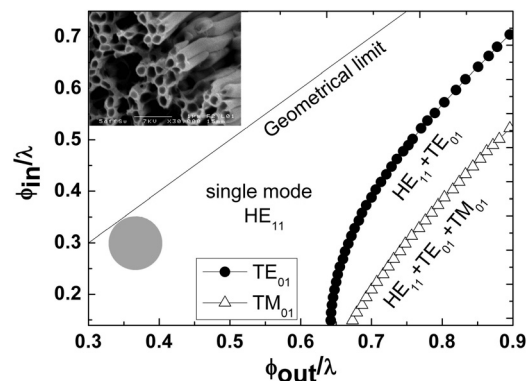


FIG. 1. Theoretical map of single mode and multimode behaviour in SU8 nanotubes as a function of inner ϕ_{in} and outer ϕ_{out} diameters normalized by the wavelength. The hatched grey zone highlights the area related to the nanotubes fabricated here ($\phi_{out} = 255$ nm and $\phi_{in} = 215$ nm). Insert: SEM image before the dispersion in single NTs.

^{a)} Author to whom correspondence should be addressed. Electronic mail: nolwenn.huby@univ-rennes1.fr.

depending on the inner diameter. The grey hatched zone highlights the area related to NTs investigated in the following section. This map clearly proves that exclusively single mode propagation exists in these SU8 nanotubes.

The propagation of light into nanotubes with appropriate diameter has been experimentally investigated. SU8 nanotubes have been elaborated and integrated onto photonic micro-chips. Their fabrication is performed by a template strategy¹³ based on the impregnation of the 200 nm-diameter pores of a commercially available 60- μm thick alumina porous membrane (anodized aluminium oxide, AAO) with a drop of SU8 photoresist. After diffusion of the SU8 in pores, the whole sample was exposed to UV light ($\lambda = 365$ nm, 200 mJ/cm²) for polymerisation. To release the nanotubes from the alumina membrane, the sample was immersed in a selective NaOH solution (1.5 M). Energy dispersive x-ray spectroscopy analysis (not shown here) confirms the total removal of the AAO. The insert in Fig. 1 displays a scanning electron microscopy (SEM) image after the removal of the sample. From a statistical analysis of SEM images, the outer diameter ϕ_{out} of SU8 nanotubes is evaluated at 255 ± 30 nm and the wall thickness at 40 ± 10 nm, which is consistent with the grey hatched zone of Fig. 1. Finally, the NTs are dispersed in single objects by sonication in isopropanol.

SU8 NTs have been integrated on a photonic integrated chip along organic SU8 microstructures. The fabrication process consists in a one-step UV-lithography process. The thickness of the microstructures (ridge waveguides of 6 μm width and microdisk of 200 μm -radius connected to ridge waveguides) is 30 μm and is determined by the viscosity of the SU8 (SU8-2025, $\eta = 4500$ Pa s) and by the patterning steps conditions.¹⁶ The final integrated photonic circuit is fully organic except the substrate working as the lower cladding layer ($n_{\text{SiO}_2} = 1.45$). Schemes of the chip and of the micro-injection bench for optical characterization are presented in Fig. 2. The optical chip is tested on a set-up based on an end-fire method to couple light from the laser into the cleaved waveguide end facets. Visible light ($\lambda = 670$ nm) and near infrared light ($\lambda = 840$ nm) have been injected. Injection is controlled and optimized with a CCD camera at the exit of the chip, as shown on the CCD image where the cross-section of a waveguide during light propagation is presented. A micro-beam profiler (MBP, Newport) equipped by a CCD camera is placed on top of the bench allowing far-field intensity record.

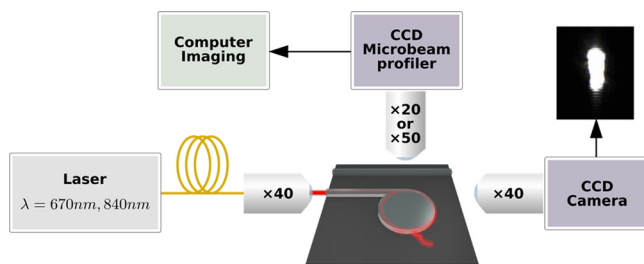


FIG. 2. (Color online) Sketch of the optical characterization set-up. Injection in integrated microstructures is optimized within cross-section imaging by a CCD camera (the CCD image shows the output of a waveguide of 30 μm high and 6 μm width). Top views of far field images are recorded with a CCD microbeam profiler.

Optical propagation in NTs is investigated through their excitation by evanescent coupling¹⁷ with a microdisk. In this purpose, light is coupled into a waveguide and propagates to the microdisk where whispering gallery modes (WGMs) are excited and circulate at the surface. This configuration is particularly appropriate since the evanescent tail of the guided light is highly dependent of the waveguide geometry. For a curved waveguide and as a consequence for a microdisk, the Gaussian beam axis shifts towards the outside of the bend¹⁸ and leads to an extended evanescent tail¹⁹ in the low refractive index medium (here, the air). Figure 3(a) shows a SEM image of a single NT located close to a microdisk. Figure 3(b) is the corresponding far-field intensity CCD image under infrared light injection. This close-up view, obtained with a 50x objective, demonstrates that light is confined both at the edges of the microdisk highlighting the WGM and along the NT. Figure 3(c) is an intensity profile plotted along the dotted white line visible in Fig. 3(b). The hatched rectangle has been added to depict the dimension of the nanotube. This profile shows the light confinement centered along the NT demonstrating the efficient optical evanescent coupling and the light propagation in these sub-wavelength nanostructures. It also highlights the high evanescent tail. Indeed, the fit of the profile with a Gaussian function leads to a full half width maximum of 739 nm. The diameter of the NT of interest being 300 nm that leads to an extension of the field slightly higher than 200 nm outwards the NT.

The scattering losses have been quantitatively estimated from the exponential attenuation coefficient α of the Beer-Lambert law $I(x) = I_0 e^{-\alpha x}$, where I is the recorded light intensity along the propagation length x (originating at the extremity of the NT close from the disk) and I_0 is the initial light intensity. Figure 3(d) shows the linear dependence $\ln I = f(x)$ along the NT during infrared light injection. The linear fit of the experimental data in Fig. 3(d) leads to losses of 210 dB/mm for infrared light. The same study has been performed under red light injection and gives 129 dB/mm. This

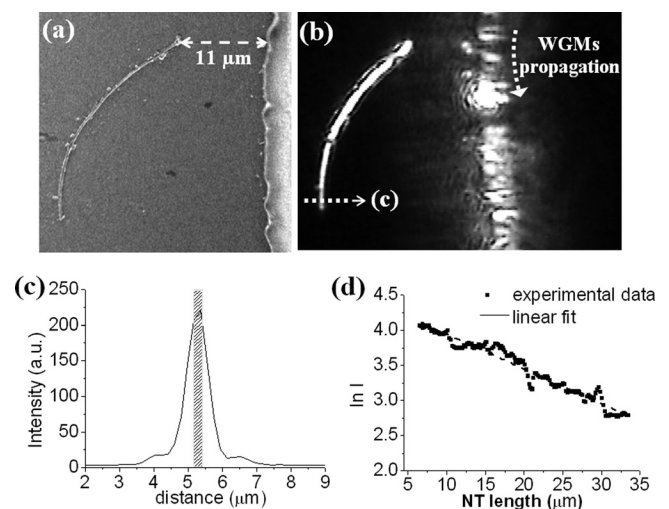


FIG. 3. (a) SEM image of a nanotube close to the edge of a disk-reservoir. (b) MBP image of the optical field during light injection. (c) Light intensity I profile along the dotted line shown in (b). The hatched rectangle represents the NT diameter. (d) Experimental plot of $(\ln I)$ as a function of the distance along the NT. The slope of the linear fit leads to scattering losses estimation.

wavelength dependence is consistent with previous studies evidenced in SU8 structures at a microscale. For magnitude losses comparison, SU8 microstructures exhibit few tenths of dB/mm (Ref. 20) for red light. Higher losses in sub-wavelength waveguiding structures are expected due to the significant evanescent field. It can be noted that plasmon waveguides²¹ present losses of few thousands dB/mm and O'Carroll *et al.* reported losses of 480 dB/mm in an active polymer nanowire waveguide.²²

In conclusion, we have demonstrated the waveguiding properties of dielectric organic nanotubes. The theoretical study predicts a HE₁₁ monomode behaviour without frequency cut-off. Integration of SU8 NTs on an organic photonic chip constituted of appropriate microstructures for efficient evanescent coupling confirms their propagation capacity with acceptable losses compared to sub-wavelength nanostructures. The features of these SU8 nanotubes make them candidates for optical interconnections in highly packed and low-cost integrated optical circuits.

The authors thank A. Carré for technical support as well as J. Le Lannic for SEM images. These works were supported by Region Bretagne and Pays de la Loire, ANR-08-JCJC-0136-01 programs and C'Nano Nord-Ouest network.

¹K. Schmitt, K. Oehse, G. Sulz, and C. Hoffmann, *Sensors* **8**, 711 (2008).

²Y. Li and L. Tong, *Opt. Lett.* **33**, 303 (2008).

³Y. Huang, X. Duan, and C. M. Lieber, *Small* **1**, 142 (2005).

⁴W. T. Hammond and J. Xue, *Appl. Phys. Lett.* **97**, 073302 (2010).

⁵Z. Hu, B. Muls, L. Gence, D. A. Serban, J. Hofkens, S. Melinte, B. Nysten, S. Demoustier-Champagne, and A. M. Jonas, *Nano Lett.* **7**, 3639 (2007).

⁶A. Krishnan, C. J. Regan, L. Grave de Peralta, and A. A. Bernussi, *Appl. Phys. Lett.* **97**, 231110 (2010).

⁷J. J. Ju, S. K. Park, S. Park, J. Kim, M.-S. Kim, M.-H. Lee, and J. Y. Do, *Appl. Phys. Lett.* **88**, 241106 (2006).

⁸M. Steinhart, J. H. Wendorff, A. Greiner, R. B. Wehrspohn, K. Nielsch, J. Schilling, J. Choi, and U. Gösele, *Science* **296**, 1997 (2002).

⁹M. Steinhart, J. H. Wendorff, and R. B. Wehrspohn, *Chem. Phys. Chem.* **4**, 1171 (2003).

¹⁰F. Massuyeau, J. L. Duvail, J. M. Lorcy, S. Lefrant, J. Wery, and E. Faulques, *Nanotechnology* **20**, 155701 (2009).

¹¹D. H. Park, B. H. Kim, M. G. Jang, K. Y. Bae, and J. Joo, *Appl. Phys. Lett.* **86**, 113116 (2005).

¹²J. Scheuer and A. Yariv, *J. Eur. Opt. Soc.* **1**, 06007 (2006).

¹³M. De Vittorio, M. T. Todaro, T. Stomeo, R. Cingolani, R. D. Cojoc, and E. Di Fabrizio, *Microelectron. Eng.* **73**, 388 (2004).

¹⁴T. Kondo, S. Juodkazis, and H. Misawa, *Appl. Phys. A* **81**, 1583 (2005).

¹⁵D. Duval and B. Bêche, *J. Opt.* **12**, 075501 (2010).

¹⁶B. Bêche, N. Pelletier, E. Gaviot, R. Hierle, A. Gouillet, J. P. Landesman, and J. Zyss, *Microelectron. J.* **37**, 421 (2006).

¹⁷D. Mulin, M. Spajer, D. Courjon, F. Carcenac, and Y. Chen, *J. Appl. Phys.* **87**, 534 (2000).

¹⁸E. G. Neumann, *IEEE Proc.* **129**, 278 (1982).

¹⁹H. Nishihara, M. Haruna, and T. Suhara, in *Optical Integrated Circuits* (McGraw-Hill, New York, 1989), p. 43.

²⁰M. Nordström, D. A. Zauner, A. Boisen, and J. Hübner, *J. Lightwave Technol.* **25**, 1284 (2007).

²¹M. Hochberg, T. Baehr-Jones, C. Walker, and A. Scherer, *Opt. Express* **12**, 5481 (2004).

²²D. O'Carroll, I. Lieberwirth, and G. Redmond, *Small* **3**, 1178 (2007).